

# Flux Synthesis, Crystal Structure, and Photoluminescence of a Heterometallic Uranyl-Europium Germanate with U=O–Eu Linkage: $K_4[(UO_2)Eu_2(Ge_2O_7)_2]$

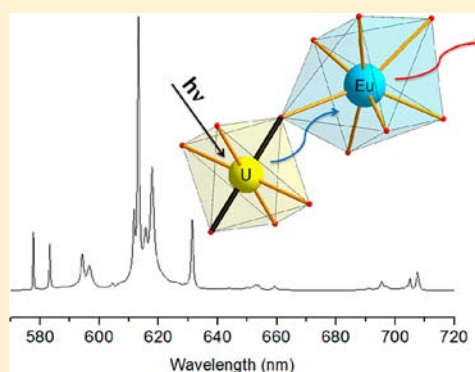
Shih-Pu Liu,<sup>†</sup> Meng-Ling Chen,<sup>†</sup> Bor-Chen Chang,<sup>\*,†</sup> and Kwang-Hwa Lii<sup>\*,†,‡</sup>

<sup>†</sup>Department of Chemistry, National Central University, Jhongli, Taiwan 32001, R.O.C.

<sup>‡</sup>Institute of Chemistry, Academia Sinica, Taipei, Taiwan 115, R.O.C.

## Supporting Information

**ABSTRACT:** Crystals of a uranyl-europium germanate,  $K_4[(UO_2)Eu_2(Ge_2O_7)_2]$ , have been grown at high temperature from a  $KF-MoO_3$  flux and structurally characterized by single-crystal X-ray diffraction. The structure contains  $PaCl_5$ -type chains formed of edge-sharing  $EuO_7$  pentagonal bipyramids that are connected by digermanate groups such that layers of europium germanate are formed. Neighboring layers are further linked by  $UO_6$  tetragonal bipyramids through uranyl ion oxygen atoms to generate a 3D framework with 6-ring channels where the  $K^+$  cations are located. The structure contains an unusual heterometallic  $U=O-Eu$  linkage. Photoluminescence studies show strong red emission at room temperature. The relative intensities of the  ${}^5D_0 \rightarrow {}^7F_1$  and  ${}^5D_0 \rightarrow {}^7F_2$  transitions confirm that the europium site lacks an inversion center. All of the emission lines show similar decay curves, which can be well-fitted by a single exponential decay function with radiative lifetimes of  $0.53 \pm 0.03$  ms. No emission is observed in the region from 450 to 550 nm typical of the uranyl cation, indicating that, upon uranyl excitation, the energy is either transferred to the  $Eu^{3+}$  centers or lost to nonradiative processes.



## INTRODUCTION

We have been interested in the exploratory synthesis of new silicates and germanates of lanthanides and uranium with novel crystal structures and interesting properties by high-temperature, high-pressure hydrothermal and flux-growth reactions. Lanthanide-containing compounds are interesting luminescent materials because they emit over the entire spectral range as near-infrared ( $Nd^{3+}$ ,  $Er^{3+}$ ), red ( $Eu^{3+}$ ,  $Pr^{3+}$ ,  $Sm^{3+}$ ), green ( $Er^{3+}$ ,  $Tb^{3+}$ ), and blue ( $Tm^{3+}$ ,  $Ce^{3+}$ ). However, luminescence from lanthanides is inherently weak. One way to enhance the intensity is to use a chromophore as a ligand, which strongly absorbs radiation energy at a suitable wavelength and then can transfer energy to excite the lanthanide to its emissive state.<sup>1</sup>

The structural chemistry of uranium silicates and germanates is particularly interesting. A large number of uranyl compounds, including an organically templated uranyl silicate, have been synthesized.<sup>2</sup> Uranyl compounds characteristically have an intense green to yellowish-green fluorescence under UV light. The luminescence emission spectra of most  $UO_2^{2+}$  compounds are mostly similar.<sup>3</sup> Usually,  $U(V)$  in solution disproportionates to  $U(IV)$  and  $U(VI)$  rapidly, precluding the formation of  $U(V)$  compounds by hydrothermal synthesis. However, we have synthesized several  $U(V)$  silicates and germanates under high-temperature, high-pressure hydrothermal conditions.<sup>4</sup> Although  $U(IV)$  is more common, few  $U(IV)$  silicates and germanates had been reported.<sup>5</sup> Recently, we reported the first synthetic

$U(IV)$  silicate,  $Cs_2USi_6O_{15}$ , whose structure is closely related to that of  $Cs_2ThSi_6O_{15}$  and several neodymium and zirconium silicates and germanates.<sup>6a</sup> A  $U(IV)$  germanate,  $Cs_4UGe_8O_{20}$ , which has a new structure and contains four- and five-coordinate germanium, was also synthesized.<sup>6b</sup> In addition, several mixed-valence uranium silicates and germanates, including uranium(IV,V), -(IV,VI), -(V,VI), and -(IV,V,VI), have been synthesized.<sup>7</sup> All mixed-valence uranium silicates and germanates with oxidation states of uranium from +4 to +6 have been observed.

Recently, Knope et al. reported the synthesis of several heterometallic  $UO_2^{2+}/Ln^{3+}$  carboxyphosphonates under mild hydrothermal conditions.<sup>8</sup> Luminescence studies of the  $U-Sm$  compound show very bright visible and near-IR  $Sm^{3+}$ -centered emission upon excitation of the uranyl moiety. No emission was observed in the region typical of the uranyl cation, indicating that all energy is either transferred to the  $Sm^{3+}$  center or lost to nonradiative processes. There are also several reports of using  $Eu^{3+}$  in a similar fashion.<sup>9</sup> The energy transfer from uranyl to  $Eu^{3+}$  ion is so efficient that the emissions from  $Eu^{3+}$  are greatly enhanced. To study uranyl sensitization of lanthanide emission, we aimed to synthesize heterometallic  $UO_2^{2+}/Ln^{3+}$  silicates and germanates that have not been reported in the literature.

Received: December 22, 2012

Published: March 18, 2013

Herein, we report the flux synthesis, single-crystal X-ray structure, and luminescence properties of the first example of uranyl lanthanide germanate,  $K_4[(UO_2)Eu_2(Ge_2O_7)_2]$  (denoted as **1**), with heterometallic  $U^{VI}=O-Eu^{III}$  cation–cation interactions.

## EXPERIMENTAL SECTION

**Synthesis.** Crystals of **1** were grown from a KF-MoO<sub>3</sub> flux. A mixture of KF (0.25 g, 4.3 mmol), MoO<sub>3</sub> (0.25 g, 1.7 mmol), UO<sub>3</sub> (0.006 g, 0.02 mmol), Eu<sub>2</sub>O<sub>3</sub> (0.074 g, 0.21 mmol), and GeO<sub>2</sub> (0.050 g, 0.48 mmol) was placed in a platinum crucible, heated to 950 °C, and isothermed for 48 h, followed by slow cooling to 750 °C at 2 °C/h, and then furnace cooled to room temperature. The flux was dissolved with hot water, and a mixture of colorless crystals of GeO<sub>2</sub>, some red block crystals of poor quality, and some light yellow block crystals of **1** was obtained. The yield of **1** was not estimated because it is very difficult to separate all the light yellow crystals from the other products. We have not been able to improve the yield from the KF-MoO<sub>3</sub> flux despite many attempts. A qualitative energy-dispersive X-ray analysis of several light yellow crystals confirmed the presence of K, U, Eu, and Ge. After crystal structure analysis, a single-phase powder product of **1** was prepared quantitatively by heating a pressed pellet of reaction mixture containing stoichiometric UO<sub>3</sub>, Eu<sub>2</sub>O<sub>3</sub>, GeO<sub>2</sub>, and KNO<sub>3</sub> (K/U/Eu/Ge mole ratio = 4:1:2:2) at 1100 °C for 10 h with an intermittent grinding, as indicated by powder X-ray diffraction (Supporting Information, Figure S1). Powder diffraction data were collected in the range of  $5^\circ \leq 2\theta \leq 50^\circ$  on a Shimadzu XRD-6000 powder diffractometer using  $\theta$ - $2\theta$  mode in a Bragg–Brentano geometry. The sample was used for photoluminescence study.

**Single-Crystal X-ray Diffraction.** A light yellow crystal of **1** having dimensions of  $0.12 \times 0.10 \times 0.06$  mm was selected for indexing, and intensity data were collected on a Bruker Kappa Apex II CCD diffractometer equipped with a normal focus, 3 kW sealed tube X-ray source. Intensity data were collected at 296 K over 1319 frames with  $\varphi$  and  $\omega$  scans (width  $0.5^\circ$ /frame) and an exposure time of 10 s/frame. Determination of integrated intensities and unit cell refinement were performed using the SAINT program.<sup>10</sup> The SADABS program was used for absorption correction ( $T_{\min}/T_{\max} = 0.490/0.746$ ).<sup>11</sup> On the basis of statistical analysis of intensity distribution and successful solution and refinement of the structure, the space group was determined to be  $P\bar{1}$  (No. 2) with lattice constants of  $a = 6.9491(4)$  Å,  $b = 6.9502(4)$  Å,  $c = 9.9102(5)$  Å,  $\alpha = 94.695(2)^\circ$ ,  $\beta = 98.659(2)^\circ$ ,  $\gamma = 110.512(2)^\circ$ , and  $V = 438.47(4)$  Å<sup>3</sup>. The structure was solved by direct methods and successive difference Fourier syntheses. Two K atom sites were located. The multiplicities of both K atoms were allowed to vary but did not deviate significantly from full occupancy. The final cycles of least-squares refinement including atomic coordinates and anisotropic thermal parameters for all atoms converged at  $R_1 = 0.0148$ ,  $wR_2 = 0.0331$  for 2098 reflections with  $I > 2\sigma(I)$ ,  $GOF = 1.100$ ,  $\rho_{\max,\min} = 0.88$ , and  $-0.72$  e-Å<sup>-3</sup>. All calculations were performed using the SHELXTL, version 6.14, software package.<sup>12</sup> The crystallographic data are given in Table 1 and selected bond distances in Table 2.

**Photoluminescence Measurements.** A powder sample of **1** was contained in a glass capillary for luminescence study. Various excitation wavelengths (305, 365, 385, 455, 473, and 532 nm) from lasers or light-emission diodes (LED) were employed as the light source to excite the powder sample for recording the emission spectra. The emission was collected by an  $f/1$  focal lens and imaged onto a monochromator (Acton Research Corporation SP2300i) attached with a photomultiplier tube (PMT, Hamamatsu R636-10). To reduce the interference of incident light scattering, a long-pass wavelength filter was inserted in front of the monochromator. This setup was also used for the measurements of emission radiative lifetime except the light source was replaced by a pulsed Nd:YAG laser (Spectra Physics INDI-40-10) beam at 532 nm. For recording the excitation spectrum, a xenon lamp was adopted as the light source, and its light was focused onto the monochromator. The wavelength-selected output was refocused to excite the sample, and its photoluminescence was imaged onto the photomultiplier tube with a 610 nm band-pass filter for

**Table 1.** Crystallographic Data for  $K_4[(UO_2)Eu_2(Ge_2O_7)_2]$

chemical formula	Eu <sub>2</sub> Ge <sub>4</sub> K <sub>4</sub> O <sub>16</sub> U <sub>2</sub>
formula weight	1244.71
cryst syst	triclinic
space group	$P\bar{1}$ (No. 2)
$a/\text{Å}$	6.9491(4)
$b/\text{Å}$	6.9502(4)
$c/\text{Å}$	9.9102(5)
$\alpha/\text{deg}$	94.695(2)
$\beta/\text{deg}$	98.659(2)
$\gamma/\text{deg}$	110.512(2)
$V/\text{Å}^3$	438.47(4)
$Z$	1
$T, ^\circ\text{C}$	23
$\lambda(\text{Mo } K\alpha), \text{Å}$	0.71073
$D_{\text{calc}}, \text{g}\cdot\text{cm}^{-3}$	4.714
$\mu(\text{Mo } K\alpha), \text{mm}^{-1}$	24.02
$R_1^a$	0.0148
$wR_2^b$	0.0331

$$^a R_1 = \sum ||F_o| - |F_c|| / \sum |F_o|. \quad ^b wR_2 = [\sum w(F_o^2 - F_c^2)^2 / \sum w(F_o^2)^2]^{1/2}, \quad w = 1/[\sigma^2(F_o^2) + (aP)^2 + bP], \quad P = [\text{Max}(F_o^2, 0) + 2(F_c^2)]/3, \quad \text{where } a = 0.0115 \text{ and } b = 0.72.$$

**Table 2.** Selected Bond Lengths (Å) for  $K_4[(UO_2)Eu_2(Ge_2O_7)_2]^a$

U(1)–O(1)	2.205(2) (2×)	U(1)–O(7)	2.240(2) (2×)
U(1)–O(8)	1.852(2) (2×)	Eu(1)–O(2)	2.245(2)
Eu(1)–O(3)	2.281(2)	Eu(1)–O(5)	2.304(2)
Eu(1)–O(5)	2.473(2)	Eu(1)–O(6)	2.324(2)
Eu(1)–O(6)	2.558(2)	Eu(1)–O(8)	2.570(2)
Ge(1)–O(1)	1.752(2)	Ge(1)–O(2)	1.720(2)
Ge(1)–O(3)	1.726(2)	Ge(1)–O(4)	1.806(2)
Ge(2)–O(4)	1.783(2)	Ge(2)–O(5)	1.732(2)
Ge(2)–O(6)	1.734(2)	Ge(2)–O(7)	1.736(2)

<sup>a</sup>Note: K–O distances are available in the Supporting Information.

monitoring the Eu<sup>3+</sup> emission. Therefore, an excitation spectrum can be obtained by scanning the monochromator.

## RESULTS AND DISCUSSION

**Structure.** The structure of **1** consists of the following distinct structural elements: one UO<sub>6</sub> tetragonal bipyramid, one EuO<sub>7</sub> polyhedron, two GeO<sub>4</sub> tetrahedra, and two K sites. U(1) is at an inversion center, and all the other atoms are in general positions. The UO<sub>6</sub> tetragonal bipyramid has two short U–O bonds (U(1)=O, 1.852(2) Å (2×)), forming the linear uranyl unit [O=U=O]<sup>2+</sup>, as is typical for U<sup>6+</sup> in crystal structures, and four longer U–O bonds (2.205(2)–2.240(2) Å) in the plane normal to the UO<sub>2</sub> axis. The bond-valence parameters  $R_{ij} = 2.074$  Å and  $b = 0.554$  Å for [6]U<sup>6+</sup> polyhedra were used to calculate the bond-valence sum at the uranium site,<sup>13</sup> and the value for U(1) was 6.05 valence units. When the optimal parameters for all types of U<sup>6+</sup> polyhedra  $R_{ij} = 2.051$  Å and  $b = 0.519$  Å was used,<sup>13</sup> the value was 5.81. Both calculation results indicate that the uranium atom is hexavalent. The uranyl ion bond lth in **1** is a little longer than the average bond length of 1.816(50) Å for a large number of uranyl square bipyramidal polyhedra in the literature.<sup>13</sup> The Eu atom is 7-fold coordinated in the +3 oxidation state, as indicated by the value of the bond-valence sum (3.12 valence units),<sup>14</sup> and the EuO<sub>7</sub> unit approximates to a pentagonal bipyramid. As shown in Figure 1a, each EuO<sub>7</sub> polyhedron shares two equatorial edges with two

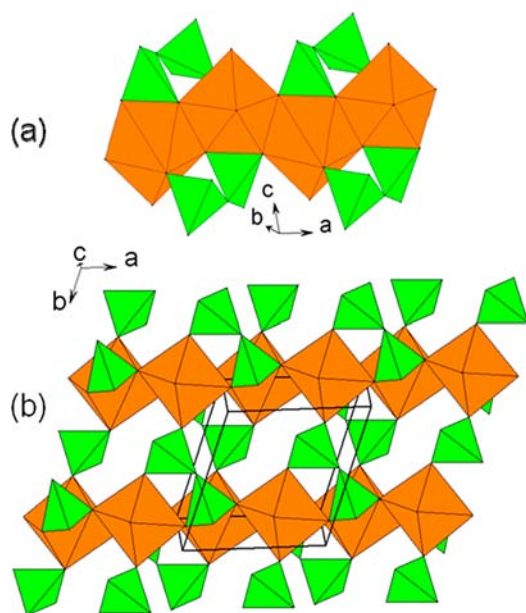


**Figure 1.** (a) Section of an infinite chain of edge-sharing  $\text{EuO}_7$  pentagonal bipyramids in **1** showing the connectivity between  $\text{EuO}_7$  and  $\text{GeO}_4$  units. (b) Section of a  $[\text{Eu}(\text{Ge}_2\text{O}_7)]$  layer viewed in a direction approximately parallel to the  $c$  axis.

$\text{EuO}_7$  polyhedra to form an infinite chain with the composition  $\text{EuO}_{2/1}\text{O}_{4/2}\text{O}_{1/1}$  (i.e.,  $\text{EuO}_5$ ) along the  $a$  axis. The chain, which is similar to that in  $\text{PaCl}_5$ , was also observed in the structures of the mixed-anion double-layer lanthanide silicates  $\text{Rb}_2\text{REGa-Si}_4\text{O}_{12}$  ( $\text{RE} = \text{Y}, \text{Eu}, \text{Gd}, \text{Tb}$ ).<sup>15,16</sup> Adjacent  $\text{Eu}-\text{O}$  chains are connected by digermanate groups such that layers with the composition  $[\text{Eu}(\text{Ge}_2\text{O}_7)]$  in the  $ab$  plane are formed (Figure 1b). Neighboring layers are linked by  $\text{UO}_6$  tetragonal bipyramids through uranyl ion oxygen atoms, O(8), to generate a 3D framework with two types of 6-ring channels parallel to the  $a$  axis where the  $\text{K}^+$  cations are located (Figure 2). The  $\text{U}=\text{O}-\text{Eu}$  bond angle is  $144.9(1)^\circ$ . Every  $\text{GeO}_4$  tetrahedron shares a corner with another tetrahedron to form a digermanate unit, with the bond angle at the bridging oxygen atom, O(4), being equal to  $129.8(1)^\circ$ . The  $\text{Ge}(1)\text{O}_4$  tetrahedron shares two corners with two  $\text{EuO}_7$  polyhedra belonging to two adjacent chains and the third corner with one  $\text{UO}_6$ .  $\text{Ge}(2)\text{O}_4$  shares an edge with one  $\text{EuO}_7$  and a corner with one  $\text{UO}_6$ . On the basis of the maximum cation–anion distance by Donnay and Allmann,<sup>17</sup> a limit of 3.35 Å was set for  $\text{K}-\text{O}$  interactions; both  $\text{K}^+$  cations are 7-coordinate. The bond-valence sums for  $\text{K}^+$  cations are 1.16 and 0.80 for  $\text{K}(1)$  and  $\text{K}(2)$ , respectively.  $\text{K}(1)$  is more tightly bonded in the structural channel, as indicated by shorter  $\text{K}-\text{O}$  distances and nearly isotropic thermal vibrations.

Cation–cation interactions (CCIs) occur when a uranyl oxygen atom is coordinated to a second uranyl cation in the equatorial position. CCIs are rare in compounds that exclusively contain  $\text{U}^{\text{VI}}$  but are much more common in pentavalent actinyl chemistry.<sup>18</sup> Such an interaction occurs in a pentavalent uranium silicate,  $\text{K}(\text{UO})\text{Si}_2\text{O}_6$ .<sup>4a</sup> The structure of **1** contains an unusual  $\text{U}=\text{O}-\text{Eu}$  linkage that is the so-called heterometallic CCIs associating  $4f$  and  $5f$  metals. Only a few compounds featuring  $\text{U}^{\text{VI}}=\text{O}-\text{Ln}^{\text{III}}$  interactions have been described,<sup>19</sup> although CCIs between  $\text{UO}_2^{2+}$  and transition metals are more common.<sup>20</sup> The longer uranyl ion bond length in **1** can be ascribed to the  $\text{U}=\text{O}-\text{Eu}$  linkage.

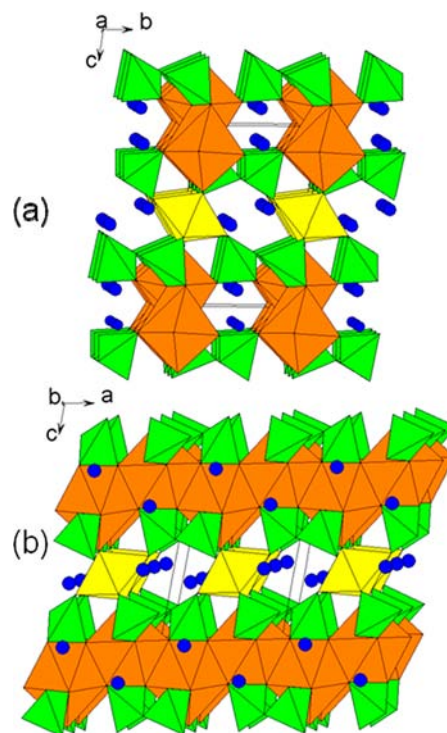


**Figure 2.** Structure of **1** viewed along (a) the  $a$  axis and (b) the  $b$  axis.

**Photoluminescence Study.** It appeared that the red emission from compound **1** was stronger than the other europium silicates or germanates synthesized by us in recent years. Figure 3 shows the room-temperature (RT) photo-

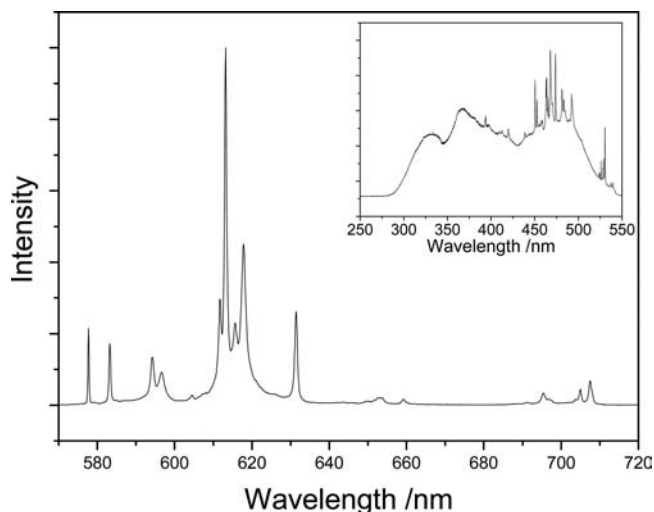


**Figure 3.** Room-temperature emission spectrum of **1** excited at 473 nm. The inset shows the excitation spectrum upon monitoring the  $\text{Eu}^{3+}$  emission at 610 nm.

luminescence emission spectrum of **1**. The excitation spectrum of **1** from 250 to 550 nm is also depicted in the inset of Figure 3. In the excitation spectrum, the sharp lines correspond to the  $\text{Eu}^{3+}$  intra- $4f^6$  transitions, including the  $^5\text{D}_{1-4} \leftarrow ^7\text{F}_0$ ,  $^5\text{L}_6 \leftarrow ^7\text{F}_0$ , and  $^5\text{G}_J \leftarrow ^7\text{F}_0$  transitions. An excitation spectrum of  $\gamma\text{-UO}_3$  was also recorded for comparison, and most of the broad bands in the inset of Figure 3 can be assigned to the uranyl ( $\text{UO}_2^{2+}$ ) transitions except the broad band at approximately 325 nm.

The band at about 325 nm could arise from the charge transfer between the uranyl oxygen and  $\text{Eu}^{3+}$ .<sup>21</sup> Since the excitation spectrum was recorded with monitoring the  $\text{Eu}^{3+}$  emission, the inset of Figure 3 clearly shows that the uranyl excitation could yield the  $\text{Eu}^{3+}$  emission, that is, the energy transfer from uranyl to  $\text{Eu}^{3+}$ . From the excitation spectrum, one could also see that the combination of strong uranyl absorption and efficient energy transfer from uranyl to  $\text{Eu}^{3+}$  can dramatically increase the  $\text{Eu}^{3+}$  photoluminescence. Furthermore, no emission is observed in the region from 450 to 550 nm typical of uranyl cation. It indicates that, upon uranyl excitation, the energy is either transferred to the  $\text{Eu}^{3+}$  centers or lost to nonradiative processes. This is similar to a previous study of the uranyl sensitization of  $\text{Sm}^{3+}$  luminescence in a coordination polymer.<sup>8</sup> Our results confirm that the uranyl sensitization is an efficient method for increasing the photoluminescence intensity as well as broadening the excitation wavelength range for compounds containing trivalent lanthanides.

The RT emission spectrum recorded at 473 nm ( $^5\text{D}_0 \leftarrow ^7\text{F}_0$ ) excitation exhibits a number of peaks between 575 and 720 nm. These peaks are ascribed to emission from the first excited  $^5\text{D}_0$  state to the  $^7\text{F}_{0-4}$  Stark levels of the fundamental  $\text{Eu}^{3+}$  septet. Although the luminescence intensities appear different because different light sources, including dye laser, diode laser, and light-emitting diode, were used, the relative intensities and frequencies of the observed lines in the emission spectra at different excitation wavelengths (305, 365, 385, 455, and 532 nm) are roughly identical to the spectrum depicted in Figure 3 due to very fast nonradiative relaxations in the excited electronic states. Because of the limited quantity of **1** and the sensitivity limit of the available instrument, we were unable to measure the luminescence quantum yield. In Figure 3, the  $^5\text{D}_0 \rightarrow ^7\text{F}_{1,3}$  transitions in the 583–598 nm and 648–660 nm regions have magnetic dipole (MD) character, whereas the  $^5\text{D}_0 \rightarrow ^7\text{F}_{2,4}$  transitions in the 610–625 nm and 690–710 nm regions have electric dipole (ED) character and are allowed due to the lack of an inversion center at the  $\text{Eu}^{3+}$  site. In contrast to the nearly equal integrated intensity between the  $^5\text{D}_0 \rightarrow ^7\text{F}_1$  and  $^5\text{D}_0 \rightarrow ^7\text{F}_2$  transitions in  $\text{Cs}_3\text{EuSi}_6\text{O}_{15}$ ,<sup>22</sup> the integrated intensity of the  $^5\text{D}_0 \rightarrow ^7\text{F}_2$  (ED) transition is much larger than that of the  $^5\text{D}_0 \rightarrow ^7\text{F}_1$  (MD) transition in **1**. The  $^5\text{D}_0 \leftarrow ^7\text{F}_0$  transition at 578 nm is quite strong and has no splitting. These results are consistent with the crystal structure of **1** where there is only one unique  $\text{Eu}^{3+}$  site without an inversion symmetry center.

We also measured the emission radiative lifetimes of strong peaks in the RT emission spectrum following the 532 nm excitation ( $^5\text{D}_1 \leftarrow ^7\text{F}_0$ ). Figure 4 illustrates that all of these emission peaks show similar decay curves, which can be well-fitted by a single exponential decay function with radiative lifetimes of  $0.53 \pm 0.03$  ms. These results confirm that all of the strong peaks in Figure 3 originate from the same upper state ( $^5\text{D}_0$ ). On the other hand, it is quite interesting that the emission in **1** shows a much shorter lifetime of approximately 0.5 ms in comparison with the value (5.45 ms) in  $\text{Cs}_3\text{EuSi}_6\text{O}_{15}$ ,<sup>22</sup> but this shorter lifetime is similar to that observed in  $\text{K}_5\text{Eu}_2\text{FSi}_4\text{O}_{13}$  (~1.7 ms) or in  $\text{KEuGe}_2\text{O}_6$  (~1 ms).<sup>23,24</sup> Since **1** does not contain any quenching group, such as hydroxyl group or water molecule, the quenching effect should play no part in these luminescence decays. Although the  $\text{Eu}^{3+}$ – $\text{Eu}^{3+}$  distance in **1** is only 3.87 Å, the concentration quenching effect is unlikely accountable for this short radiative lifetime because the  $\text{Eu}^{3+}$ – $\text{Eu}^{3+}$  distance is 3.85 Å in  $\text{KEuGe}_2\text{O}_6$ <sup>24</sup> and our experiments

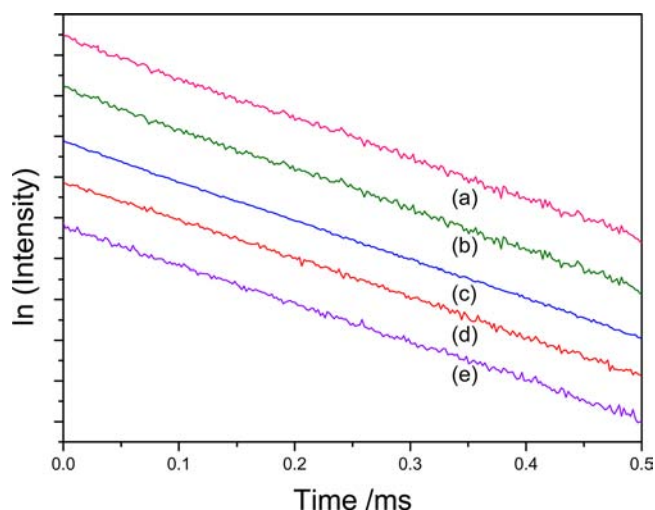


**Figure 4.** Luminescence decays at natural log scale vs time at different emission wavelengths: (a) 578, (b) 583, (c) 613, (d) 618, and (e) 632 nm.

show no evidence of concentration quenching in  $\text{KEuGe}_2\text{O}_6$ . On the other hand, the shorter emission lifetime implies a larger electronic transition dipole moment in **1**, and this is supported by its very strong photoluminescence emission. The larger transition dipole moment may be attributed to the anisotropy of electron density of the  $\text{Eu}^{3+}$  4f orbitals. For example, the  $\text{Eu}^{3+}$  site in  $\text{Cs}_3\text{EuSi}_6\text{O}_{15}$ <sup>22</sup> is in a relatively regular octahedral field with six similar Eu–O bonds, whereas in  $\text{K}_5\text{Eu}_2\text{FSi}_4\text{O}_{13}$ ,<sup>23</sup>  $\text{Eu}^{3+}$  is located in the center of a distorted octahedron with five Eu–O bonds and one Eu–F bond and, therefore, has larger anisotropy of electron density. The  $\text{Eu}^{3+}$  site in  $\text{KEuGe}_2\text{O}_6$ <sup>24</sup> naturally has a large anisotropy of electron density since it is in the center of a distorted pentagonal bipyramid. Moreover, in the present case, there exists heterometallic cation–cation interaction between  $\text{UO}_2^{2+}$  and  $\text{Eu}^{3+}$ . The  $\text{U}=\text{O}$ – $\text{Eu}$  linkage could significantly increase the anisotropy of electron density and result in a much larger transition dipole moment with a very strong photoluminescence.

In summary, a heterometallic uranyl-europium germanate has been synthesized from a  $\text{KF}\cdot\text{MoO}_3$  flux. The unique structure contains infinite chains of edge-sharing  $\text{EuO}_7$  pentagonal bipyramids and an unusual  $\text{U}=\text{O}$ – $\text{Eu}$  linkage. The luminescence properties have also been reported. The compound shows very bright red emission at room temperature. The relative intensities of  $^5\text{D}_0 \rightarrow ^7\text{F}_1$  and  $^5\text{D}_0 \rightarrow ^7\text{F}_2$  transitions are in agreement with the crystallographic results, and the emission lifetime measurements confirm the presence of one local  $\text{Eu}^{3+}$  environment. The very short lifetime can be ascribed to the large anisotropy of electron density of the  $\text{Eu}^{3+}$  4f orbitals that may arise from the heterometallic cation–cation interactions. Energy transfer from uranyl to europium was found to be very efficient with strong broad-band uranyl sensitization from 300 to 550 nm. This is the first example of a uranyl lanthanide germanate. Further research to synthesize 4f–5f heterometallic silicates and germanates with interesting crystal structures and properties by the flux-growth and high-temperature, high-pressure hydrothermal methods is in progress.

## ■ ASSOCIATED CONTENT

### ■ Supporting Information

The X-ray crystallographic data of **1** in CIF format and PXRD patterns. This material is available free of charge via the Internet at <http://pubs.acs.org>.

## ■ AUTHOR INFORMATION

### Corresponding Author

\*E-mail: [liikh@cc.ncu.edu.tw](mailto:liikh@cc.ncu.edu.tw) (K.-H.L.), [bchang@ncu.edu.tw](mailto:bchang@ncu.edu.tw) (B.-C.C.).

### Notes

The authors declare no competing financial interest.

## ■ ACKNOWLEDGMENTS

We thank the National Science Council of Taiwan for financial support.

## ■ REFERENCES

- (1) Cotton, S. *Lanthanide and Actinide Chemistry*; Wiley: Chichester, U.K., 2006.
- (2) (a) Wang, X.; Huang, J.; Liu, L.; Jacobson, A. J. *J. Mater. Chem.* **2002**, *12*, 406–410. (b) Chen, C.-S.; Kao, H.-M.; Lii, K.-H. *Inorg. Chem.* **2005**, *44*, 935–940. (c) Lin, C.-H.; Chiang, R.-K.; Lii, K.-H. *J. Am. Chem. Soc.* **2009**, *131*, 2068–2069. (d) Ling, J.; Morrison, J. M.; Ward, M.; Poinssatte-Jones, K.; Burns, P. C. *Inorg. Chem.* **2010**, *49*, 7123–7128. (e) Morrison, J. M.; Moore-Shay, L. J.; Burns, P. C. *Inorg. Chem.* **2011**, *50*, 2272–2277.
- (3) Hanchar, J. M. Spectroscopic Techniques Applied to Uranium in Minerals. In *Uranium: Mineralogy, Geometry and the Environment*; Burn, P. C., Finch, R., Eds.; Reviews in Mineralogy; Mineralogical Society of America: Washington, DC, 1999; Vol. 38, pp 499–519.
- (4) (a) Chen, C.-S.; Lee, S.-F.; Lii, K.-H. *J. Am. Chem. Soc.* **2005**, *127*, 12208–12209. (b) Lin, C.-H.; Chen, C.-S.; Shiryaev, A. A.; Zubavichus, Y. V.; Lii, K.-H. *Inorg. Chem.* **2008**, *47*, 4445–4447. (c) Nguyen, Q. B.; Chen, C.-L.; Chiang, Y.-W.; Lii, K.-H. *Inorg. Chem.* **2012**, *51*, 3879–3882.
- (5) (a) Stieff, L. R.; Stern, T. W.; Sherwood, A. M. *Science* **1955**, *121*, 608–609. (b) Stieff, L. R.; Stern, T. W.; Sherwood, A. M. *Am. Mineral.* **1956**, *41*, 675–688. (c) Durif, P. A. *Acta Crystallogr.* **1956**, *9*, 533. (d) Uvarova, Y. A.; Sokolova, E.; Hawthorne, F. C.; Agakhanov, A. A.; Pautov, L. A. *Can. Mineral.* **2004**, *42*, 1005–1011.
- (6) (a) Liu, H.-K.; Lii, K.-H. *Inorg. Chem.* **2011**, *50*, 5870–5872. (b) Nguyen, Q. B.; Lii, K.-H. *Inorg. Chem.* **2011**, *50*, 9936–9938.
- (7) (a) Lin, C.-H.; Lii, K.-H. *Angew. Chem., Int. Ed.* **2008**, *47*, 8711–8713. (b) Lee, C.-S.; Wang, S.-L.; Lii, K.-H. *J. Am. Chem. Soc.* **2009**, *131*, 15116–15117. (c) Lee, C.-S.; Lin, C.-H.; Wang, S.-L.; Lii, K.-H. *Angew. Chem., Int. Ed.* **2010**, *49*, 4254–4256. (d) Nguyen, Q. B.; Liu, H.-K.; Chang, W.-J.; Lii, K.-H. *Inorg. Chem.* **2011**, *50*, 4241–4243.
- (8) Knope, K. E.; de Lill, D. T.; Rowland, C. E.; Cantos, P. M.; de Bettencourt-Dias, A.; Cahill, C. L. *Inorg. Chem.* **2012**, *51*, 201–206.
- (9) (a) Okamoto, Y.; Ueba, Y.; Nagata, I.; Banks, E. *Macromolecules* **1981**, *14*, 807–809. (b) Tanner, S. P.; Vargenas, A. R. *Inorg. Chem.* **1981**, *20*, 4384–4386. (c) Lopez, M.; Birch, D. J. S. *J. Lumin.* **1997**, *71*, 221–228. (d) Seregina, E. A.; Seregin, A. A.; Tikhonov, G. V. *J. Alloys Compd.* **2002**, *341*, 283–287. (e) Maji, S.; Viswanathan, K. S. *J. Lumin.* **2009**, *129*, 1242–1248.
- (10) Sheldrick, G. M. *SAINT*, Version 7.68A; University of Göttingen: Göttingen, Germany, 2009.
- (11) Sheldrick, G. M. *SADABS*, Version 2008/1; University of Göttingen: Göttingen, Germany, 2008.
- (12) Sheldrick, G. M. *SHELXTL Programs*, Version 6.14; Bruker AXS GmbH: Karlsruhe, Germany, 2000.
- (13) (a) Burns, P. C.; Ewing, R. C.; Hawthorne, F. C. *Can. Mineral.* **1997**, *35*, 1551–1570. (b) Burns, P. C. In *Structural Chemistry of Inorganic Actinide Compounds*; Krivovichev, S. V., Burns, P. C.,

Tananaev, I. G., Eds.; Elsevier: Amsterdam, The Netherlands, 2007; Chapter 1, pp 1–30.

- (14) Brown, I. D.; Altermatt, D. *Acta Crystallogr.* **1985**, *B41*, 244–247.
- (15) Dodge, R. P.; Smith, G. S.; Johnson, Q.; Elson, R. E. *Acta Crystallogr.* **1967**, *22*, 85–89.
- (16) Lee, C.-S.; Liao, Y.-C.; Hsu, J.-T.; Wang, S.-L.; Lii, K.-H. *Inorg. Chem.* **2008**, *47*, 1910–1912.
- (17) Donnay, G.; Allmann, R. *Am. Mineral.* **1970**, *55*, 1003–1015.
- (18) (a) Sullens, T. A.; Jensen, R. A.; Shvareva, T. Y.; Albrecht-Schmitt, T. E. *J. Am. Chem. Soc.* **2004**, *126*, 2676–2677. (b) Adelan, P. O.; Burns, P. C. *Inorg. Chem.* **2012**, *51*, 11177–11183 and references cited therein.
- (19) (a) Volkringer, C.; Henry, N.; Grandjean, S.; Loiseau, T. *J. Am. Chem. Soc.* **2012**, *134*, 1275–1283. (b) Arnold, P. L.; Hollis, E.; White, F. J.; Magnani, N.; Caciuffo, R.; Love, J. B. *Angew. Chem., Int. Ed.* **2011**, *50*, 887–890.
- (20) Tian, T.; Yang, W.; Pan, Q.-J.; Sun, Z.-M. *Inorg. Chem.* **2012**, *51*, 11150–11154 and references cited therein.
- (21) Bacce, E. D.; Pires, A. M.; Davolos, M. R. *J. Alloys Compd.* **2002**, *344*, 312–315.
- (22) Huang, M.-Y.; Chen, Y.-H.; Chang, B.-C.; Lii, K.-H. *Chem. Mater.* **2005**, *17*, 5743–5747.
- (23) Chiang, P.-Y.; Lin, T.-W.; Dai, J.-H.; Chang, B.-C.; Lii, K.-H. *Inorg. Chem.* **2007**, *46*, 3619–3622.
- (24) Chen, P.-L.; Chiang, P.-Y.; Yeh, H.-C.; Chang, B.-C.; Lii, K.-H. *Dalton Trans.* **2008**, 1721–1726.